filler metal in the amorphous state for brazing of precipitation-hardened copper alloy of the Glidcop Al–25 grade provided the brazed joints with a tensile strength of 80–90 % of that of the base metal [10].

It can be concluded from the above-said that rapidly quenched brazing filler metal $Ti_{57}Cu_{43}$ in the form of a strip is X-ray amorphous. Isothermal annealing at 510 °C leads to transformation of the alloy from the amorphous state to the crystalline one, in which the δ-CuTi and γ-$CuTi_2$ crystalline structures are identified.

1. Kovneristy, Yu.K. (1999) *Volume-amorphising metal alloys*. Moscow: Nauka.
2. Khorunov, V.F., Maksymova, S.V. (2005) Amorphous filler alloys — promising material for advanced brazing processes (Review). *The Paton Welding J.*, **10**, 33–38.
3. Fatkhullin, O.Kh. (2005) State-of-the-art in metal science of rapidly quenched heat-resistant alloys. *Tekhnologiya Lyog. Splavov*, **1–4**, 24–31.
4. Kalin, B.A., Fedotov, V.T., Sevryukov, O.N. et al. (1996) Amorphous brazing filler metal strips. Experience of development of the manufacturing technology and application. *Svarochn. Proizvodstvo*, **1**, 15–19.
5. Kalin, B.A., Plyushchev, A.N., Fedotov, V.T. et al. (2001) Effect of structural state of brazing filler metal on physical-mechanical properties of brazed joints. *Ibid.*, **8**, 38–41.
6. Shpak, A.P., Kunitsky, Yu.A., Lysov, V.I. (2002) *Cluster and nanostructural materials*. Kiev: Akademperiodika.
7. Nemoshkalenko, V.V., Romanova, A.V., Iliinsky, F.G. (1987) *Amorphous metal alloys*. Kiev: Naukova Dumka.
8. Romanova, A.V. (1995) Some historical facts and memories about development of notions of atomic structure of liquid and metal glasses. *Metallofizika, Novejshie Tekhnologii*, **8**, 3–29.
9. Golder, Yu.G. (1978) Metal glasses. *Tekhnologiya Lyog. Splavov*, **6**, 74–93.
10. Maksimova, S.V., Khorunov, V.F., Shonin, V. A. et al. (2002) Vacuum brazing of dispersion-strengthened copper alloy Glidcop Al–25. *The Paton Welding J.*, **10**, 13–17.

INFLUENCE OF WORKING DISTANCE OF WELDING ELECTRON GUN ON WELD GEOMETRY

O.K. NAZARENKO and **V.I. ZAGORNIKOV**
E.O. Paton Electric Welding Institute, NASU, Kiev, Ukraine

Geometry of electron beam penetrations in a wide range of gun to workpiece distances was experimentally studied. A weak correlation was established between the gun to workpiece distance and penetration depth in thick metals. The possibility of substantially increasing of working distance without a marked change in the penetration parameters is attributable to a corresponding decrease of the convergence angle of the beam within the workpiece region.

Keywords: *electron beam gun, welding gun, working distance, weld depth, focal point, angle of beam convergence*

No international standard on spatial characteristics of welding electron beam has been introduced so far, despite a high interest to the issue of interaction of beam parameters and weld geometry [1, 2]. Focal spot dimensions, i.e. beam minimum section in the welded workpiece plane, are quite often specified in the requirements to welding electron gun. It is believed that a small spot is the main condition for formation of deep welds with minimum transverse dimensions of the cast zone and with simultaneous improvement of secondary electron image of the welding zone. As the focal spot dimensions are directly proportional to the welding gun working distance, many operators are trying to place it as close as possible to the workpiece, despite a concurrent increase of the probability of electric breakdowns in the accelerating gap of the gun, because of metal vapour and gas penetration from the weld pool.

At electron beam welding of thin metal (up to several millimetres), when surface supply of thermal energy is performed and there is practically no crater in the weld pool, dimensions of minimum beam section on the workpiece surface indeed determine the dimensions of the cast zone at other conditions being equal. However, when the weld forms in the metal of the thickness of tens and even hundreds of millimetres, focal spot dimensions proper no longer determine the cast zone dimensions, and spatial characteristics of the so-called focal depth of the beam, or, in other words, its isthmus, along the length of which the averaged specific energy density in the beam is practically constant, have a much greater role. The longer the isthmus, the easier it is to form a weld of maximum depth with practically parallel side walls. Therefore, it is correct to state that the angle of inclination of side walls of the cast zone is largely determined by the overall configuration of the beam in the isthmus region.

Experimental study of the geometry of electron beam penetrations in a broad range of welding gun working distances, the results of which are discussed below, has been performed as a stage of preparation of normative materials on equipment and technology of electron beam welding.

Experimental procedure and obtained results. Experiments were performed using ELA-60 power unit with 60 kV accelerating voltage. Schematic of electron-optic system is given in Figure 1. The gun is fitted with tablet LaB_6-cathode with radius r_{cath} = = 1.5 mm, working temperature T_{cath} = 2000 K. Middle of non-magnetic gap of the focusing electromagnetic lens is located at distance a = 120 mm from beam

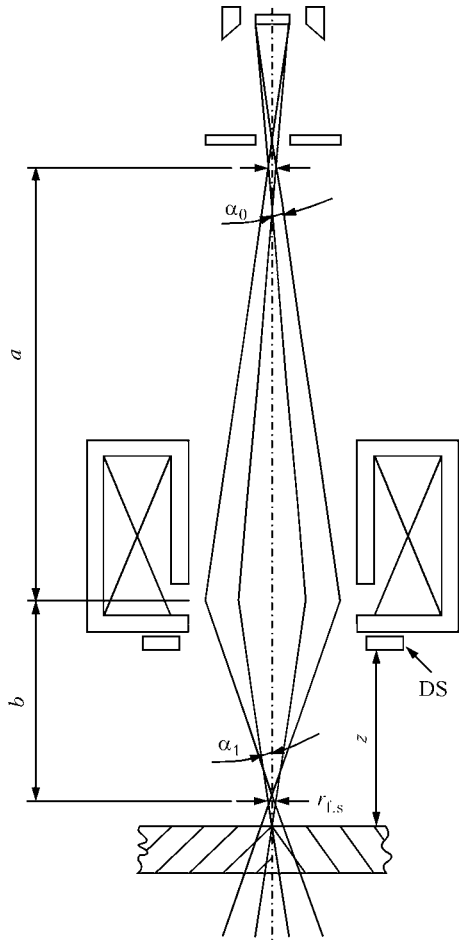

Figure 1. Schematic of electron optical system of ELA-60 gun: *a*, *b* — distances from the middle of lens non-magnetic gap to the crossover and focusing plane, respectively; α_0, α_1 — half-angles of beam divergence after the cross-over and beam convergence above the isthmus, respectively; DS — deflecting system; *z* — working distance; $r_{f.s}$ — focal spot radius

cross-over — minimum beam section at emission system outlet. Lens inner diameter $D = 40$ mm, non-magnetic gap width $S = 18$ mm.

As transverse beam dimensions considerably depend on the coefficient of spherical aberration of the lens, let us assess it using the following relationships, where lens magnification $M = b/a$ [3]:

$$\frac{C_{sph}}{S} = \left[\frac{a}{S}\right]^3 \left[1 + \frac{1}{M}\right] p(x) \left[\frac{1 + 1/M}{a/S} q(x) + 1\right], \quad (1)$$

$$x = D/S, \quad (2)$$

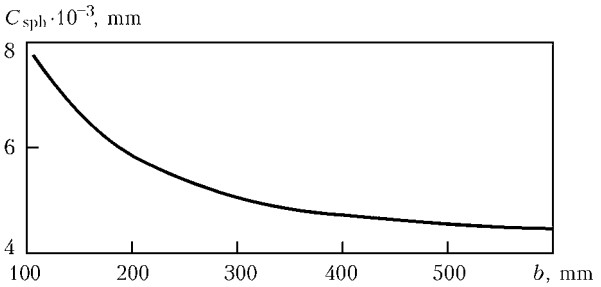

Figure 2. Calculated dependence of the coefficient of spherical aberration of magnetic lens of ELA-60 gun on non-magnetic gap–focusing plane distance

$$q(x) = 0.26x - 0.25, \quad (3)$$

$$p(x) = \frac{2.46}{x + 0.47} - 0.28. \quad (4)$$

For $b = 100$–600 mm calculated values of the coefficient of spherical aberration of the applied focusing lens C_{sph} are given in Figure 2.

Experiments were performed on plates of low-carbon steel 09G2S 65 mm thick and stainless steel 12Kh18N10T 8 mm thick. Beam focusing plane was located below plate surface at the depth of 32 and 4 mm, respectively, penetration being incomplete, and the plates proper being mounted at an angle of about 10° to the horizon with the purpose of finding the maximum depth as accurately as possible. Location of maximum penetration depth was determined by location of minimum width of the cast zone on plate surface, where sections were cut out for macrosection preparation. Thick plates were located at the following distances from gun edge: 20, 100, 220 and 470 mm, and thins ones — at distances of 45, 125, 245 and 495 mm, respectively. Values $b = 120$ mm (lens magnification $M = 1$), 220 mm ($M = 1.7$), 320 mm ($M = 2.7$) and 570 mm ($M = 4.75$) correspond to working distances in each case. Welding speed of 5 mm/s and beam power of 24 kW for 65 mm thick metal, welding speed of 25 mm/s and beam power of 4.8 kW for 8 mm metal were unchanged, U_{acc} being 60 kV in both the cases.

Figure 3 gives the obtained results for different distances to the workpiece.

Discussion of results. Obtained experimental data unambiguously point to a weak correlation of penetration depth and distance to the workpiece. At beam power of 4.8 kW just a comparatively small reduction of penetration depth is observed with increase of gun to workpiece distance from 45 up to 495 mm.

In case of application of 24 kW beam in the range of gun to workpiece distances of 200 to 600 mm the penetration depth is practically constant. At minimum distance to the workpiece of 20 mm when focal spot diameter is minimum, penetration depth turned out to be by 25 % smaller than at large working distances.

To clarify the obtained experimental results, let us perform estimation of spatial characteristics of the beam depending on its length. When making the calculations, let us proceed from the fact that beam transverse dimensions are determined by thermal velocities of electrons, spherical aberration and magnification of focusing lens. Owing to a high stability and small pulsations of power unit parameters, we will neglect the influence of chromatic aberration of the magnetic lens on beam transverse dimensions. Influence of beam volume charge is also neglectable, as it is compensated by positively charged ions near the anode opening [4].

Assuming beam radius to be the distance from beam axis to circumference line, where current density de-

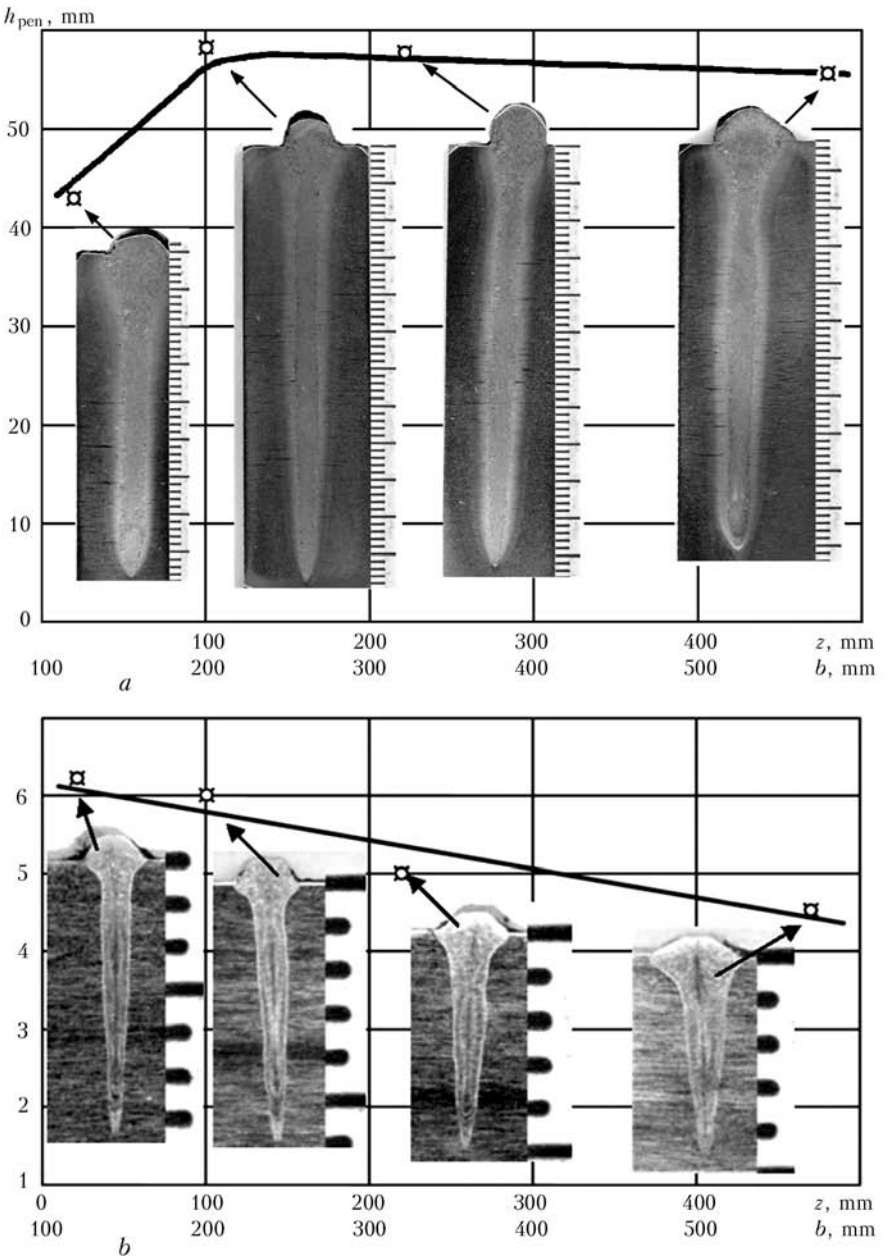

Figure 3. Change of penetration depth and transverse macrosections at different distances to the workpiece for steel 09G2S (w_b = 24 kW) (*a*) and 12Kh18N10T (48 kW) (*b*)

creases e = 2.718 times relative to current density on beam axis, according to Langmuir, we have

$$r_{cr} = r_{cath}\left\{\frac{T}{11600U_{acc}}\right\}^{0.5}\frac{1}{\alpha_0}. \quad (5)$$

If beam crossover is projected on the welded workpiece plane by a magnetic lens, free of spherical aberration, beam radius on the workpiece is equal to

$$r_1 = Mr_{cr} = r_{cath}\left\{\frac{T}{11600U_{acc}}\right\}^{0.5}\frac{1}{\alpha_1}. \quad (6)$$

If the electrons have no thermal velocities, but the lens is characterized by spherical aberration, beam radius on the workpiece is equal to

$$r_2 = (M+1)^4 C_{sph}\alpha_1^3. \quad (7)$$

In the real case, the focal spot radius can be presented as follows:

$$r_{f.s} = (r_1^2 + r_2^2)^{0.5}. \quad (8)$$

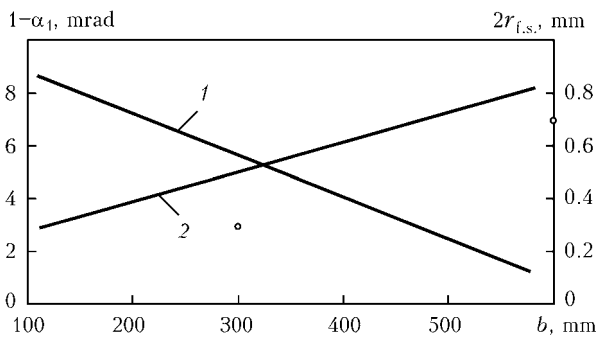

Figure 4. Calculated dependencies of half-angle of convergence (*1*) and focal spot radius (*2*) for different distances *b*

Hence we have [5]

$$\alpha_1 = 0.87 \frac{1}{M+1} \frac{r_{cath}^{0.25}(T/11600)^{0.125}}{C_{sph}^{0.25}\, U_{acc}^{0.125}}, \quad (9)$$

$$r_{f.s} = 1.33(M+1) \frac{r_{cath}^{0.75} C_{sph}^{0.25} (T/11600)^{0.375}}{U_{acc}^{0.375}}. \quad (10)$$

Results of assessment of the radius and half-angle of beam convergence in the plane of the workpiece, removed to different distances from the gun, are given in Figure 4.

As follows from Figure 4, at increase of the distance from the middle of the gun non-magnetic gap to the workpiece practically by 5 times (from 120 to 570 mm) the focal spot radius increases 3 times. However, owing to a decrease of the angle of convergence of the beam, the length of beam isthmus increases and, accordingly, the depth and geometry of the cast zone of formed penetrations changes only slightly.

A certain decrease of penetration depth at a limit small working distance is attributable to the fact that value of half-angle of beam convergence of 10^{-2} rad is critical for the experimental conditions, as the isthmus length turns out to be insufficient for formation of a deeper penetration.

CONCLUSIONS

1. While in electron beam welding of 3–4 mm thick metal geometrical dimensions of penetration are determined by cross-sectional radius of low-power electron beam, in welding thick metal by a higher-power beam, respectively, the depth of the cast zone depends on the length of beam isthmus, which is determined by the angle of convergence of the beam on the workpiece.

2. Length of the isthmus of the beam, formed by a specific welding gun, changes only lightly in a rather wide range of distances to the workpiece, therefore the cast zone depth remains practically unchanged.

3. For the most widely used welding guns of ELA-60 type of 10–60 kW power the recommended optimal distance from gun edge to the workpiece is 150–200 mm, allowing for the need for a good reflection of the butt zone in secondary electrons.

1. Menhard, C., Loewer, T. (2009) The electron beam geometry — definition, measurement and significance for the welding process. *Welding and Cutting*, 8(**3**), 138–142.
2. Mladenov, G., Koleva, E. (2007) Evaluation and some applications of the electron beam emittance. In: *Proc. of 7th Int. Conf. on Beam Technology* (17–19 April 2007, Halle, Germany), 85–92.
3. Der-Shvarts, G.V. (1971) To calculation of spherical aberration of axisymmetric magnetic lenses. *Radiotekhnika i Elektronika*, **7**, 1305–1306.
4. Nazarenko, O.K., Kajdalov, A.A., Kovbasenko, S.N. et al. (1987) *Electron beam welding*. Ed. by B.E. Paton. Kiev: Naukova Dumka.
5. Bas, E.B., Cremosnik, G., Lerch, H. (1962) Beitrag zum Problem der Erzeugung des Elektronenstrahles fuer Schmelzen. *Verdampfen, Schweissen und Rohren mit Elektronenstrahlen: Schweizer Archiv fuer angewandte Wissenschaft und Technik*, 112–121.